Nanoscale Res Lett (2010) 5:31–37
DOI 10.1007/s11671-009-9439-y

NANO EXPRESS

Growth of InAs Quantum Dots on Germanium Substrate Using Metal Organic Chemical Vapor Deposition Technique

Tanuj Dhawan · Renu Tyagi · Rajesh Kumar Bag · Mahavir Singh · Premila Mohan · T. Haldar · R. Murlidharan · R. P. Tandon

Received: 28 April 2009 / Accepted: 9 September 2009 / Published online: 19 September 2009

Abstract Self-assembled InAs quantum dots (QDs) were grown on germanium substrates by metal organic chemical vapor deposition technique. Effects of growth temperature and InAs coverage on the size, density, and height of quantum dots were investigated. Growth temperature was varied from 400 to 450 °C and InAs coverage was varied between 1.40 and 2.35 monolayers (MLs). The surface morphology and structural characteristics of the quantum dots analyzed by atomic force microscope revealed that the density of the InAs quantum dots first increased and then decreased with the amount of InAs coverage; whereas density decreased with increase in growth temperature. It was observed that the size and height of InAs quantum dots increased with increase in both temperature and InAs coverage. The density of QDs was effectively controlled by growth temperature and InAs coverage on GaAs buffer layer.

Keywords Quantum dots · Ge substrate · InAs · Self-assembled

Introduction

Self-assembled InAs quantum dots (QDs) grown on GaAs substrate have generated a momentous interest in the last few years due to their potential applications in QD lasers [1, 2] and infrared photodetectors [3, 4]. QD lasers have demonstrated superior characteristics such as ultra-low-threshold current densities [5, 6], ultra-high-temperature stability [7], very high differential efficiency [8], small α-factor, and correspondingly reduced filamentation [9]. GaAs has been the most common substrate used for the growth of InAs quantum dots although germanium (Ge) is equally interesting and promising alternative substrate material because of its almost identical lattice constant and thermal expansion coefficient to those of GaAs. Ge is cost effective and is available in large wafer sizes. Ge has higher mechanical strength than GaAs and therefore thinner Ge substrate can be used, resulting in light weight end products [10]. For GaAs substrates etch pit density (EPD) value is generally above 100/cm^2 but Ge substrates are of a perfect crystalline quality (0 EPD) [11]. This makes Ge a suitable replacement of GaAs in various above-mentioned applications.

InAs QDs grown on GaAs substrates by both molecular beam epitaxy (MBE) and metal organic chemical vapor deposition (MOCVD) techniques have been reported by several groups [12, 13], and effects of growth rate, V/III ratio, growth temperature, and material coverage on InAs QDs grown on GaAs substrate have been well studied [14]. Ge substrates have also been used for the fabrication of InGaAs/AlGaAs lasers [11] and (Al)GaInP multi-quantum well LEDs [15]. Surprisingly, there is only one report by Knuuttila et al. [16] describing the growth of non-uniformly distributed InAs islands directly on Ge substrate without any buffer layer. In the growth of InAs QDs directly on Ge substrate by Stranski–Krastanow (SK) growth mode, the formation of anti phase domains (APDs) is inevitable because the dot formation takes place after a thin wetting layer is grown. This thin wetting layer itself

T. Dhawan · R. P. Tandon (✉)
Department of Physics & Astrophysics, University of Delhi, Delhi 110007, India
e-mail: ram_tandon@hotmail.com

R. Tyagi · R. K. Bag · M. Singh · P. Mohan · T. Haldar · R. Murlidharan
Solid State Physics Laboratory, Lucknow Road, Timarpur, Delhi 110054, India

will be infested with defects. This may adversely influence the growth of good quality dots subsequently. This could be one of the possible reasons which did not allow other groups to have a successful growth of InAs quantum dots directly on Ge substrates. Moreover, APDs may be reduced to a maximum extend if a buffer layer is grown on Ge substrate. Buffer layer assists in reducing the surface defects of the substrate and helps in confining InAs QDs. However, growth of uniformly distributed InAs QDs on Ge substrate using GaAs buffer layer is scarcely reported. Motivated by the above ideas, we report the effect of growth temperature and InAs coverage on the formation of InAs QDs on Ge substrate having a GaAs buffer layer.

Experimental Details

Growth of GaAs and InAs layers was carried out using Thomas Swan horizontal MOCVD reactor. The source materials used were TMGa, TMIn, and AsH_3, and Ge (001) 6° off toward (110) substrates were used for all the growth runs. GaAs buffer layer of thickness 360 nm was grown at 660 °C and at a reactor pressure of 660 Torr. InAs quantum dots were grown for different InAs coverage and temperature. Growth temperature was varied from 400 to 450 °C and InAs coverage was varied between 1.40 and 2.35 monolayers (MLs). V/III ratio was kept at 90. Prior to growth, Ge substrates were degreased with organic solvent, then etched by an etchant $HF:H_2O_2:H_2O$ (1:1:5) for 2 mins, and finally etched in dilute HF to remove surface oxide. Prior to loading into the reactor, the substrates were dried by blowing dry N_2. Veeco Nanoscope III atomic force microscope (AFM) was used to study the topography of the grown QDs. Dot size, density, and height were also determined as a function of temperature and growth time. Crystalline quality of GaAs buffer layer grown on Ge substrate was studied using double crystal X-ray diffraction (X'Pert MRD, Philips). Optical characterizations of the samples were performed by photoluminescence (PL) measurement setup (Dongwoo) at a temperature of 77 K, using a diode laser of wavelength 532 nm. The PL signal was detected by a Si detector.

Results and Discussions

When polar material (GaAs, InAs) is epitaxially grown on non-polar material (Ge), it often leads to structural defects known as APDs which creates deep levels inside the forbidden band and acts as strong scattering centers [17, 18]. They can also result in significant surface roughness which hinders large area uniformity. The most common methods for avoiding APDs from GaAs/Ge interfaces is by deliberately using misoriented substrates [19–22] and growth using arsenic pre-layer [23]. Thickness of GaAs buffer layer is also crucial, as antiphase domains self-annihilate in a region of about 50 nm from the interface, leaving the GaAs final surface nearly free of APDs [21].

In the present study we have followed a two-step growth process to grow GaAs buffer layer, the details on growth are reported elsewhere [10]. We have used 6° off Ge substrate, grown with a GaAs buffer layer of thickness 360 nm using arsenic pre-layer. In order to ascertain crystalline quality of GaAs buffer layer grown on Ge substrate, X-ray rocking curve was studied using double crystal X-ray diffraction (Fig. 1). The CuK_α ($\lambda = 1.54$ Å) radiation was used as a source of radiation and (004) reflection was studied. Full width at half maximum (FWHM) of GaAs was found to be 36 arc sec, which is less than or comparable to the earlier reports [10, 24]. The narrowness of the FWHM of the GaAs epitaxial film peak indicates that the crystalline quality of GaAs epitaxial film is reasonably good.

In first set of experiments, growth temperature for InAs QDs was fixed at 420 °C and InAs coverage was varied between 1.40 and 2.35 MLs. Figure 2 shows the AFM images of QDs at different InAs coverage of (a) 1.4 MLs, (b) 1.80 MLs, (c) 1.85 MLs, (d) 1.95 MLs, and (e) 2.35 MLs. In SK growth mode, few monolayers of two-dimensional (2-D) growth occur prior to the QDs formation. The critical layer thickness at which this 2-D to 3-D transition occurs depends on the lattice mismatch between the layer being deposited and the substrate. For InAs layer deposited on GaAs substrate, the critical layer thickness is around 1.6 MLs. Figure 2a shows the surface morphology of sample with coverage of 1.4 MLs. At the lowest material coverage of 1.4 MLs, there is no signature of quantum dots

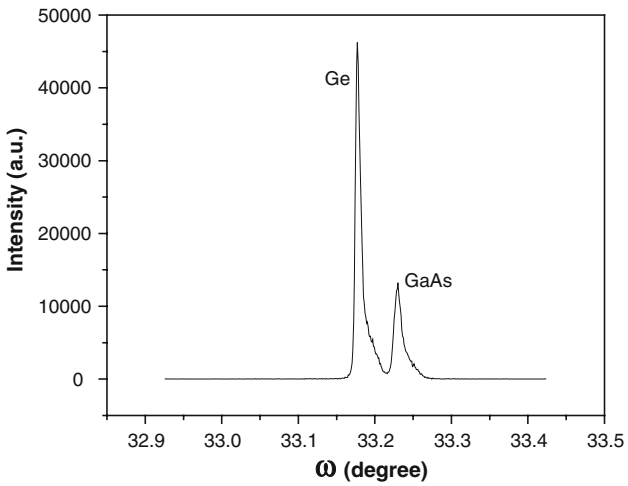

Fig. 1 DCXRD rocking curve from the (400) Bragg lines of GaAs epitaxial films grown at 660 °C on Ge substrate

and only steps on the Ge substrate are visible. This is because critical thickness has not been achieved and 2-D wetting layer is present. As we increase deposition thickness to 1.8 MLs which is above the critical thickness, QDs formation was observed with very low density of dots.

The samples with InAs coverage of 1.80 and 1.85 MLs show nearly unimodal size distribution of the dots having a dot diameter and average height of about 30 nm ± 5% and 3.0 nm ± 5%, 30 nm ± 5% and 3.9 nm ± 5%, respectively. However, the sample with InAs coverage of 1.95 MLs shows bi-modal size distribution with smaller dots having 3.3 nm ± 5% average height and 20 nm ± 5% diameter while larger dots having 5.2 nm ± 5% average height and 40 nm ± 5% diameter. Fig. 3a, b confirms that the samples with InAs coverage of 1.80 and 1.85 MLs have mono-modal size distribution whereas sample with InAs coverage of 1.95 MLs (Fig 3c) have bi-modal size distribution. In the sample shown in Fig. 2e, with InAs coverage of 2.35 MLs, the increased InAs coverage has led to coalescence for the formation of bigger islands.

Density of dots is determined from AFM images of Fig. 2. A linear growth in height of QDs was observed as a

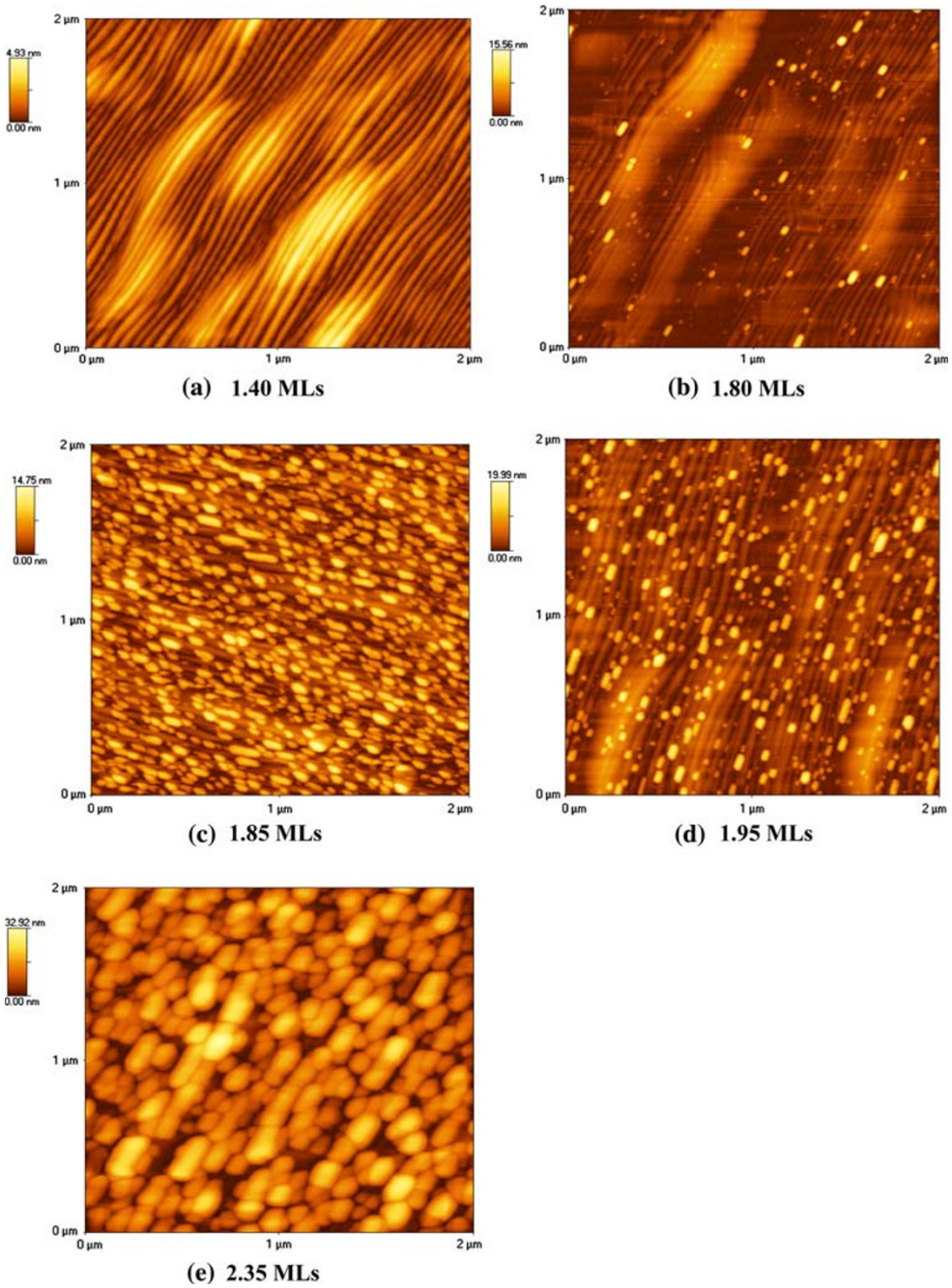

Fig. 2 AFM images of InAs QDs grown at 420 °C on Ge substrate with InAs coverage of **a** 1.4 MLs, **b** 1.80 MLs, **c** 1.85 MLs, **d** 1.95 MLs, and **e** 2.35 MLs. The scan size for all the images is 2 µm × 2 µm

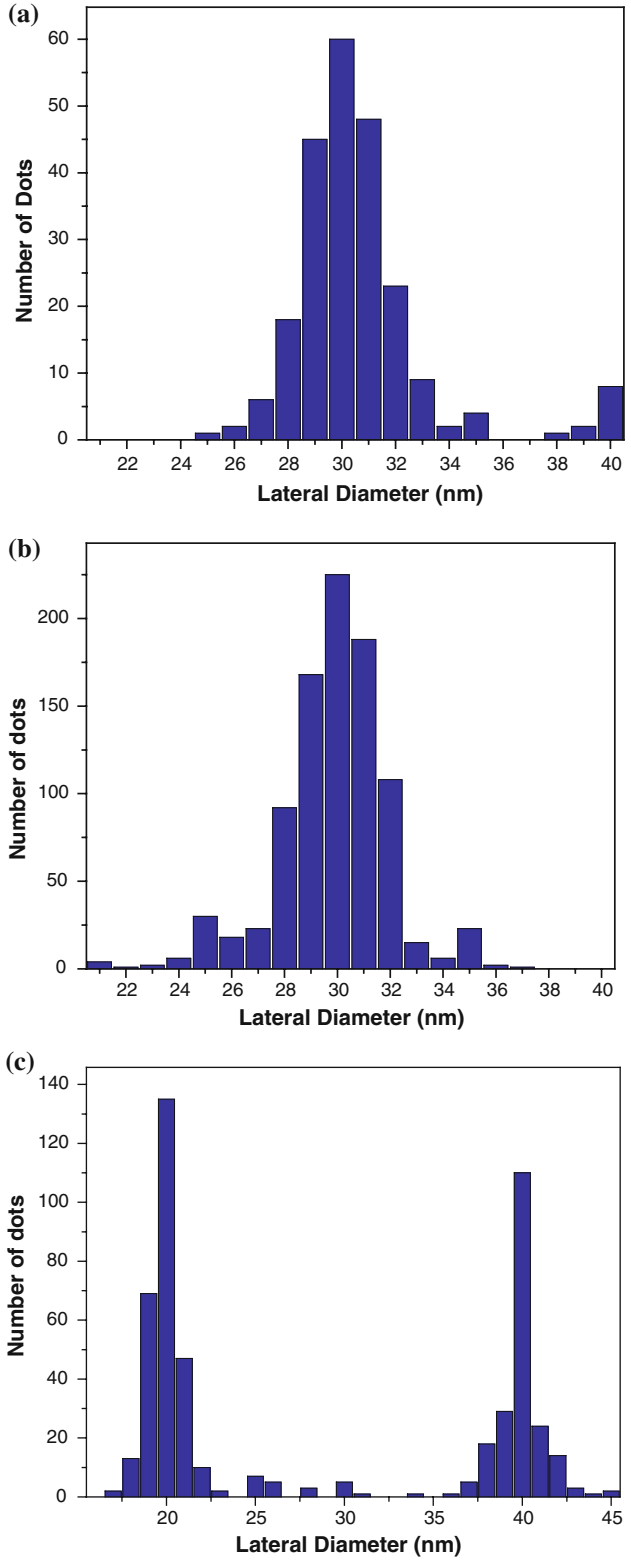

Fig. 3 Histograms of the InAs quantum dots grown at 420 °C and InAs coverage of **a** 1.80 MLs, **b** 1.85 MLs, **c** 1.95 MLs showing variation of number of dots with lateral diameter. These histograms were created from 2 μm × 2 μm AFM images

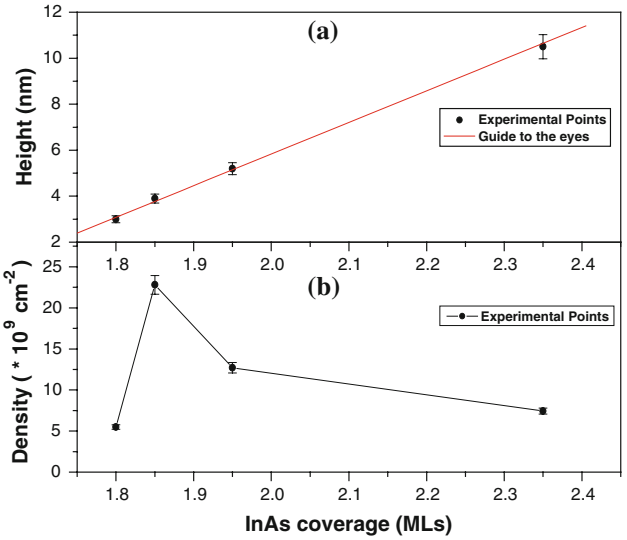

Fig. 4 The dimensional parameters, **a** height and **b** density of quantum dots as a function of InAs coverage at 420 °C

function of InAs coverage as depicted in Fig. 4a. In the initial stage of growth only very few small dots formed with large separation as can be seen from Fig. 2b resulting in a low density. As InAs coverage increases, nucleation proceeds, density of dots increases, but dots are still well separated, as in Fig. 2c. The further growth in dot size leads to decrease in density due to coalescence of QDs as shown in Fig. 4b [also, refer Fig. 2d]. The densities of QDs for InAs coverage of 1.80, 1.85, 1.95, and 2.35 MLs are 5.5×10^9, 2.28×10^{10}, 1.27×10^{10}, and 7.43×10^9 cm^{-2}, respectively. At coverage of 1.85 MLs, the size and density of the dots seem to be optimum for various possible device applications. Similar trend has been reported for InAs QDs grown on GaAs substrate [25].

The emission characteristics of the InAs QDs were determined by measuring their PL spectra at 77 K. Representative PL spectra of the sample having maximum density of dots are shown in Fig. 5. The observed PL spectra were quite broad and very much similar to that shown by Knuuttila et al. [16], although the peak energies are slightly different. Therefore, we further analyze the PL spectra by deconvolution as fitted to three distinct emission peaks (1.37, 1.33, and 1.29 eV) shown in Fig. 5. The most intense peak has the energy equal to the average of other two peak energies. The deconvolution PL spectra reflect an energy shift of the main peak by ±0.04 eV. This shift can easily be attributed to a marginal variation in dot sizes. However, it should be noted that the blue shift of QD band gap (and hence the emission energy) due to the quantum confinement is inversely proportional to the square of dot size and the effective mass of the charge carriers of the

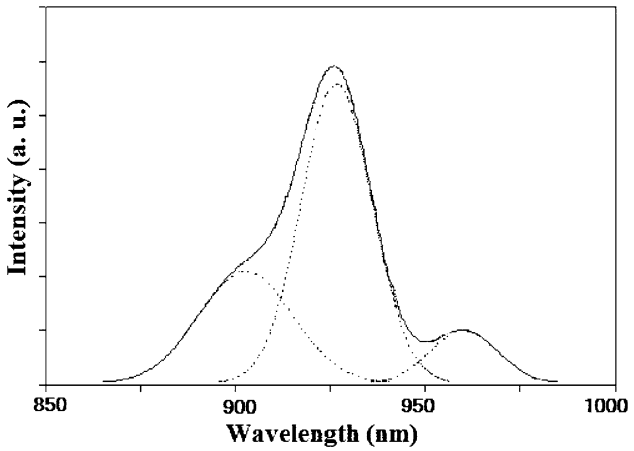

Fig. 5 PL spectra of QDs grown at 420 °C and under InAs coverage of 1.85 MLs measured at 77 K

material. Since effective mass of electron in InAs is quite small, a large blue shift is expected even for small change in dot size. The deviation of peak energy by ±0.04 eV corresponds to a deviation of dot size by ±0.1 nm for InAs in this energy range. The PL peak energy (1.33 eV) observed in the present study is greater than the earlier reported value of 1.15 eV which indicates the smaller size of QDs in our case [16]. PL peak energies of other samples were found to be consistent with their corresponding dot sizes.

Figure 6 shows the PL spectra of QDs grown at 420 °C with InAs coverage of 1.4 MLs and 1.8 MLs measured at 77 K. PL spectra of sample with InAs coverage of 1.4 MLs do not show any sign of QD formation. Only GaAs peak is visible in the spectrum. PL spectra with InAs coverage of 1.8 MLs show the QD peaks at 1.31, 1.34, and 1.36 eV. In this energy region, all three QD peaks represent almost same size. Comparing PL spectra of samples with InAs coverage of 1.80 MLs and 1.85 MLs, we find the peak positions in PL spectra of both the samples are almost same. This shows QD size is same in both the samples. This is also confirmed by the AFM studies on these samples. Both the samples differ in the density of QDs. Sample with more InAs coverage has greater density of QDs.

Temperature is one of the key parameters in the formation of QDs. It affects the adatom mobility and hence the density and size of the QDs. InAs coverage was fixed at 1.95 MLs and effect of growth temperature was investigated in the temperature range of 400 to 450 °C. For sample grown at 400 °C (Fig. 7a), shallow islands with base diameter of 40 nm ± 5% were formed. As we increased the temperature, the dots were found to change their shape significantly. At a temperature of 420 °C, spherical QDs were formed. On careful examination we found that dot height has increased with the increase in temperature. Deposited material has redistributed itself to

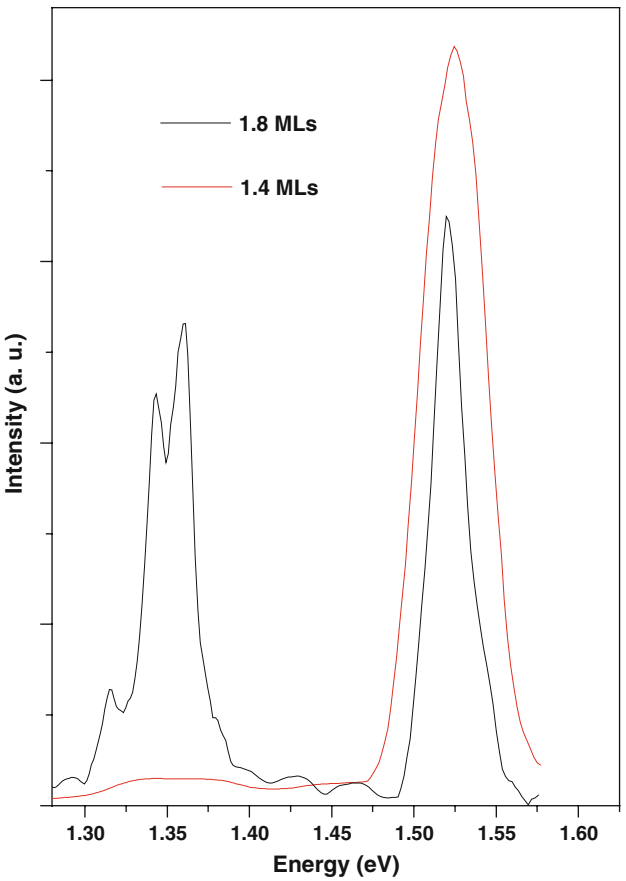

Fig. 6 PL spectra of QDs grown at 420 °C with InAs coverage of 1.4 MLs and 1.8 MLs measured at 77 K

form spherical dots (Fig. 7b). On further increase in temperature (Fig. 7c) large islands are formed due to increased surface adatom mobility.

Density of QDs decreased with increase in temperature due to coalescence of dots. Dots have coalesced due to increased adatom mobility with increase in temperature. The density of dot at 400, 420, and 450 °C was found to be 2.18×10^{10}, 1.27×10^{10}, and 3.75×10^{9} cm^{-2}, respectively. Variation of dot height and density with temperature is shown in Fig. 8. Dot height increased with the increase in temperature. The dots of average height 3.1 nm ± 5%, 3.3 nm ± 5%, and 4.9 nm ± 5% were grown at temperatures 400, 420, and 450° C, respectively. Similar variation of height and density of InAs QDs on GaAs substrate with temperature has been reported by other authors [26].

Conclusions

Self-assembled InAs QDs were grown on Ge substrates using a GaAs buffer layer. Effects of InAs coverage and growth temperature on size, height, and density of InAs QDs on Ge substrate were investigated. Height and size of

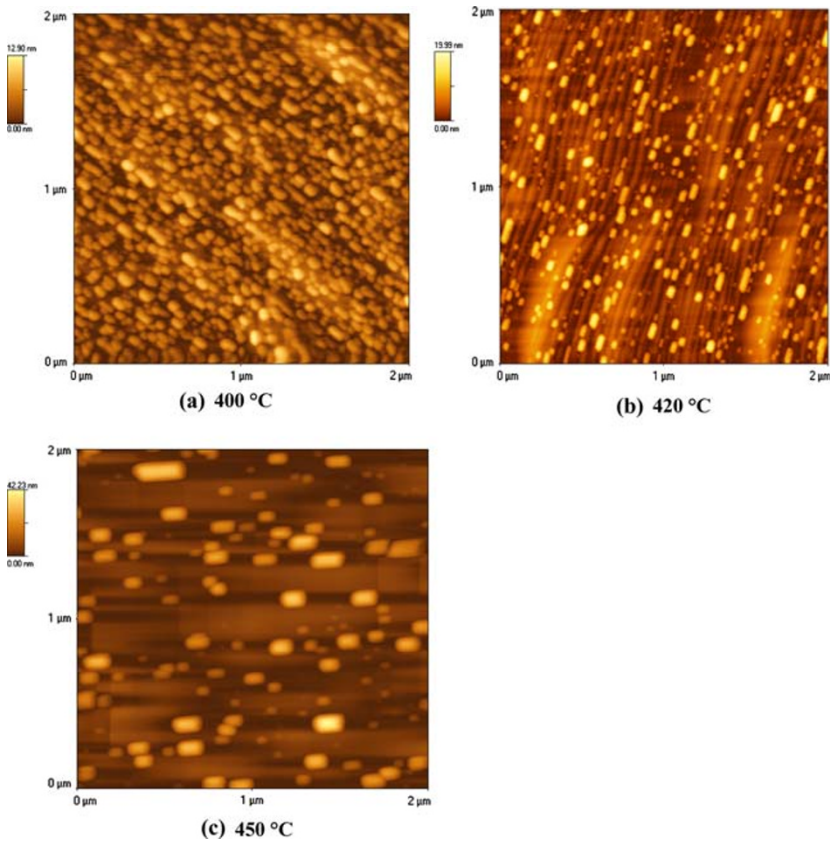

Fig. 7 AFM images of InAs QDs grown at **a** 400 °C, **b** 420 °C, **c** 450 °C, with InAs coverage of 1.95 MLs. The size of each scan is 2 μm × 2 μm

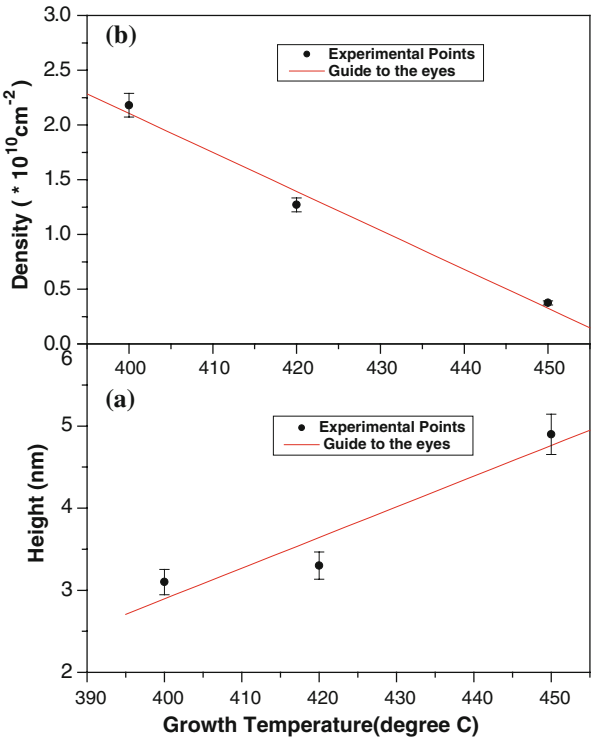

Fig. 8 The dimensional parameters, **a** height and **b** density of quantum dots as a function of growth temperature for a InAs coverage of 1.95 MLs

the QDs increased by increasing both InAs coverage and growth temperature. Density of QDs decreased with increase in growth temperature whereas in case of InAs coverage, density of dots first increased and then decreased with increase in InAs coverage. Density of QDs was effectively controlled by varying its growth temperature and amount of material deposited. The growth of good quality InAs quantum dots on Ge substrates for possible device applications is demonstrated. Hence, Ge can be used as an alternative substrate to GaAs for the successful growth of InAs QDs.

Acknowledgments Authors are thankful to Mr. Suresh Jangir, SSPL, New Delhi, for PL measurements and Dr. A. G. Vedeshwar, Department of Physics & Astrophysics, University of Delhi, for valuable discussions. Authors would also like to thank to Dr. B. R. Mehta and Dr. Deepak Varandani, IIT Delhi, for AFM measurements. One of the Authors, Tanuj Dhawan, is thankful to Director, SSPL, for providing experimental facilities and a research fellowship.

References

1. H.Y. Liu, M. Hopkinson, K. Groom, R.A. Hogg, D.J. Mowbray, Proc. SPIE Int. Soc. Opt. Eng. **6909**, 690903 (2008). doi: 10.1117/12.765735
2. Z. Mi, C. Wu, J. Yang, P. Bhattacharya, J. Vac. Sci. Technol. B Microelectron. Nanometer. Struct. **26**, 1153 (2008). doi:10.1116/1.2889386

3. D. Pal, J. Walker, E. Towe, J. Vac. Sci. Technol. B Microelectron. Nanometer. Struct. **24**, 1532 (2006). doi:10.1116/1.2190675
4. E.-T. Kim, A. Madhukara, Z. Ye, J.C. Campbell, Appl. Phys. Lett. **84**, 3277 (2004). doi:10.1063/1.1719259
5. G. Park, O.B. Shchekin, D.L. Huffaker, D.G. Deppe, IEEE Photon. Technol. Lett. **12**, 230 (2000). doi:10.1109/68.826897
6. M. Grundmann, D. Bimberg, Jpn. J. Appl. Phys. **36**, 4181 (1997). doi:10.1143/JJAP.36.4181
7. O.B. Shchekin, J. Ahn, D.G. Deppe, Electron. Lett. **38**, 712 (2002). doi:10.1049/el:20020509
8. A.R. Kovsh, N.A. Maleev, A.E. Zhukov, S.S. Mikhrin, A.R. Vasil'ev, Yu.M. Shemyakov, M.V. Maximov, D.A. Livshits, V. Ustinov, Zh.I. Alferov, N.N. Ledentsov, D. Bimberg, Electron. Lett. **38**, 1104 (2002). doi:10.1049/el:20020793
9. Ch. Ribbat, R.L. Sellin, I. Kaiander, F. Hopfer, N.N. Ledentsov, D. Bimberg, A.R. Kovsh, V.M. Ustinov, A.E. Zhukov, M.V. Maximov, Appl. Phys. Lett. **82**, 952 (2003). doi:10.1063/1.1533841
10. S.K. Aggarwal, R. Tyagi, M. Singh, R.K. Jain, Sol. Energy Mater. Sol. Cells **59**, 19 (1999). doi:10.1016/S0927-0248(99)00027-6
11. M. D'Hondt, Z.-Q. Yu, B. Depreter, C. Sys, I. Moerman, P. Demeester, P. Mijlemans, J. Cryst. Growth **195**, 655 (1998). doi:10.1016/S0022-0248(98)00652-6
12. M. Hjiri, F. Hassen, H. Maaref, Mater. Sci. Eng. B **69–70**, 514 (2000). doi:10.1016/S0921-5107(99)00248-2
13. Y. Lee, E. Ahn, J. Kim, P. Moon, C. Yang, E. Yoon, H. Lim, H. Cheong, Appl. Phys. Lett. **90**, 033105 (2007). doi:10.1063/1.2432285
14. A.A. El-Emawy, S. Birudavolu, P.S. Wong, Y.B. Jiang, H. Xu, S. Huang, D.L. Huffaker, J. Appl. Phys. **93**, 3529 (2003). doi:10.1063/1.1543647
15. P. Modak, M. D'Hondt, P. Mijlemans, I. Moerman, P. Van Daele, P. Demeester, J. Electron. Mater. **29**, 80 (2000)
16. L. Knuuttila, K. Kainu, M. Sopanen, H. Lipsanen, J. Mater. Sci. Mater. Electron. **14**(5–7), 349 (2003). doi:10.1023/A:1023992432393
17. H. Kroemer, J. Cryst. Growth **81**, 193 (1987). doi:10.1016/0022-0248(87)90391-5
18. P.M. Petroff, J. Vac. Sci. Technol. B **4**, 874 (1986)
19. Y. Li, L. Lazzarini, L.J. Giling, G. Salviati, J. Appl. Phys. **76**, 5748 (1994). doi:10.1063/1.358412
20. L. Lazzarini, L. Nasi, G. Salviati, C.Z. Fregonara, Y. Li, L.J. Giling, C. Hardingham, D.B. Holt, Micron **31**, 217 (2000). doi:10.1016/S0968-4328(99)00086-4
21. W. Li, S. Laaksonen, J. Haapamaa, M. Pessa, J. Cryst. Growth **227–228**, 104 (2001). doi:10.1016/S0022-0248(01)00641-8
22. Y. Li, G. Salviati, M.M.G. Bongers, L. Lazzarini, L. Nasi, L.J. Giling, J. Cryst. Growth **163**, 195 (1996). doi:10.1016/0022-0248(95)00958-2
23. R. Tyagi, M. Singh, M. Thirumavalavan, T. Srinivasan, S.K. Aggarwal, J. Electron. Mater. **31**(3), 234 (2002)
24. M.K. Hudait, S.B. Krupanidhi, J. Appl. Phys. **89**, 5972 (2001). doi:10.1063/1.1368870
25. H.H. Tan, K. Sears, S. Mokkapati, L. Fu, Y. Kim, P. McGowan, M. Buda, C. Jagdish, IEEE J. Sel. Top. Quantum Electron. **12**, 1242 (2006). doi:10.1109/JSTQE.2006.882663
26. Z.M. Wang, *Self-Assembled Quantum Dots* (Springer, 2008)